



# Structure-Based Design and Protein X-ray Analysis of a Protein Kinase Inhibitor

Pascal Furet,<sup>a,\*</sup> Thomas Meyer,<sup>a</sup> André Strauss,<sup>b</sup> Sylvie Raccuglia<sup>b</sup>  
and Jean-Michel Rondeau<sup>b,\*</sup>

<sup>a</sup>Novartis Pharmaceuticals Inc., Oncology Research, CH-4002 Basel, Switzerland

<sup>b</sup>Novartis Pharmaceuticals Inc., Core Technologies, CH-4002 Basel, Switzerland

Received 27 August 2001; revised 9 October 2001; accepted 24 October 2001

**Abstract**—A 5-aryl-1H-pyrazole molecular scaffold was designed to ligate the ATP binding site of cyclin dependent kinase 2 (CDK2) on the basis of crystallographic information. A search of the compound collection of Novartis using this scaffold as substructure query led to the identification of PKF049-365 as a representative of a new class of inhibitors of the cell cycle kinases CDK1/2. The three-dimensional structure of CDK2 in complex with PKF049-365 was subsequently determined by protein crystallography and refined to 1.53 Å resolution. The X-ray analysis confirmed the binding mode expected from the design hypothesis. In addition, it revealed an alternative binding orientation involving a second tautomeric form of the inhibitor that was not envisaged during the design stage. © 2002 Elsevier Science Ltd. All rights reserved.

## Introduction

In contemporary pharmaceutical research, massive screening remains the principal approach to lead finding. However, when the structural determinants of the desired biological activity are well understood, an alternative lead identification process not relying on brute force and requiring the testing of a much smaller number of compounds can be envisaged. In this respect, a possible approach is the design, by interactive molecular modeling, of chemical scaffolds judiciously chosen to make favorable interactions with the parts of the targeted binding site that are known to be critical for ligand affinity. The designed scaffolds can then lead to the synthesis of prototype molecules or serve as substructure queries in compound database searches.<sup>1</sup> In the present letter, we wish to illustrate this approach to lead finding by reporting our work on the structure-based identification and characterization by protein X-ray crystallography, of the pyrazole compound PKF049-365 as a new CDK1/2 kinase inhibitor.

## Design

Analysis of the many available crystal structures of kinase/inhibitor complexes reveals the existence of con-

served interactions that appear to be determinant for the recognition of small heterocyclic molecules by the ATP (cofactor) binding site of this class of enzymes.<sup>2</sup> Prominent among these are hydrogen bond interactions that inhibitors make with the backbone of the amino acid stretch that connects the kinase N- and C-terminal domains, the so called ‘hinge’ loop. In particular, for CDK2, at least one hydrogen bond with hinge residue Leu 83 is observed in all reported crystal structures.<sup>3</sup> These hydrogen bonds position the inhibitors in an orientation that allow them to make multiple favorable contacts with the side chains of hydrophobic residues that normally form the environment of the adenine ring of ATP in the pocket. In the case of CDK2, these residues include Ile 10, Ala 31, Val 64, Phe 80, Leu 134 and Ala 144. Recognizing the importance of the hinge hydrogen bonds and the associated hydrophobic interactions to obtain binding affinity for the ATP pocket, our strategy to find new kinase inhibitors is based on the design of molecular scaffolds targeting these interactions.

As an illustration of this approach, we used an X-ray crystal structure of CDK2 to design<sup>4</sup> a 5-aryl-1H-pyrazole ligand scaffold in the following way (Fig. 1):

- a pyrazole ring was constructed both to form bidentate hydrogen bonds with the backbone

\*Corresponding authors. E-mail: pascal.furet@pharma.novartis.com; (P. Furet); jeanmichel.rondeau@pharma.novartis.com (J. Rondeau).

carbonyl and NH groups of hinge residue Leu 83 and make hydrophobic contacts with the side chain of Leu 134.

- an aryl moiety was attached at position 5 of the pyrazole ring to create hydrophobic interactions with the side chain of Ile 10.
- finally, the 3-position of the pyrazole ring was substituted by a hydrophobic group such as phenyl or isopropyl to fill the bottom of the pocket formed by the side chains of Ala 31, Val 64, Phe 80 and Ala 144. In the model, the phenyl substituent appeared particularly interesting because, unlike a shorter group, it could make contacts with Phe 80, the residue having the deepest location in the pocket.

### Database Searching and Biological Results

Following the design, we searched the compound collection of Novartis employing the substructure query shown in Figure 2.<sup>5</sup> The search returned several compounds available for testing. All of them had a phenyl moiety in position 3 of the pyrazole ring. The retrieved compounds were tested for their ability to inhibit the

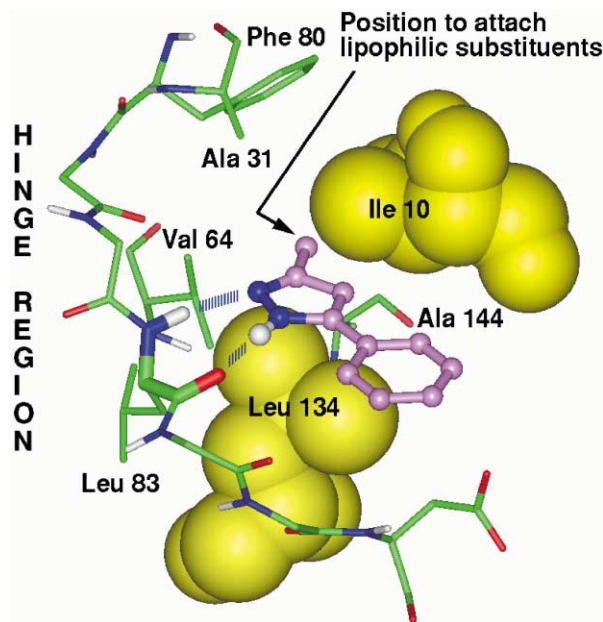


**Figure 1.** Designed scaffold in the ATP pocket of CDK2. Hydrogen bonds to Leu 83 are indicated as dashed lines.

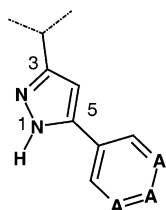


**Figure 2.** Substructure query used in the database search (A means a carbon or a nitrogen atom and the dashed lines any type of bond).

enzymatic activity of CDK2 (activated by cyclin A),<sup>6</sup> as well as that of CDK1 (activated by cyclin B)<sup>7</sup> which has a very similar ATP binding site.<sup>8</sup> Some of the compounds turned out to inhibit both enzymes with  $IC_{50}$  values in the low micromolar range. With an  $IC_{50}$  value of 1.6  $\mu$ M against CDK2 and of 1.3  $\mu$ M against CDK1, PKF049-365 (Fig. 3) was the most active one.<sup>9</sup> This result clearly demonstrated the validity of our approach in the search for new chemical series of kinase inhibitors.

### X-ray Analysis

The three-dimensional structure of the CDK2/PKF049-365 complex was determined by protein crystallography and refined to 1.53 Å resolution (Table 1).<sup>10</sup> The X-ray analysis shows that PKF049-365 binds to the adenine pocket of the ATP binding site and interacts with the hinge region of the kinase molecule, as designed by molecular modeling (Fig. 4). However, two overlapping—and hence mutually exclusive—binding modes are detected, which are characterized by a different pattern of hydrogen-bonded interactions with the main chain of the hinge region of the kinase. In the first binding mode, which corresponds exactly to the design hypothesis, N2 of the pyrazole ring of PKF049-365 receives a H-bond from the amide nitrogen of Leu 83 and N1 donates a H-bond to the carbonyl oxygen of the

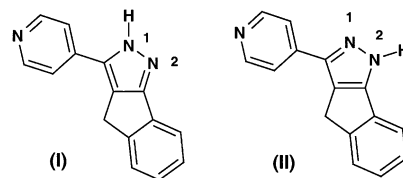


**Figure 3.** Two tautomeric forms of PKF049-365. The first one corresponds to the structure recorded in the database and identified by the search.

**Table 1.**

Crystal data	
Space group	P2 <sub>1</sub> 2 <sub>1</sub> 2 <sub>1</sub>
Unit cell dimensions	53.53, 71.80, 72.36 Å
Number of complexes/a.u.	1
Resolution range	30.0–1.53 Å
Number of observations	179,814
Number of unique reflections	39,979
Data redundancy	4.5
Data completeness	93.5%
<I/σ(I)>	14.0
R <sub>merge</sub>	0.046
Refinement statistics	
R <sub>cryst</sub>	0.206
R <sub>free</sub>	0.253
Nb of non-H protein atoms	2409
Nb of non-H ligand atoms	36 (2×18)
Nb of solvent molecules	267
mean B value for protein	23.2 Å <sup>2</sup>
mean B value for ligand	19.4 Å <sup>2</sup>
mean B value for waters	34.5 Å <sup>2</sup>
C–V estimated coord. error	0.22 Å
Rmsd bond lengths	0.008 Å
Rmsd bond angles	1.7 °

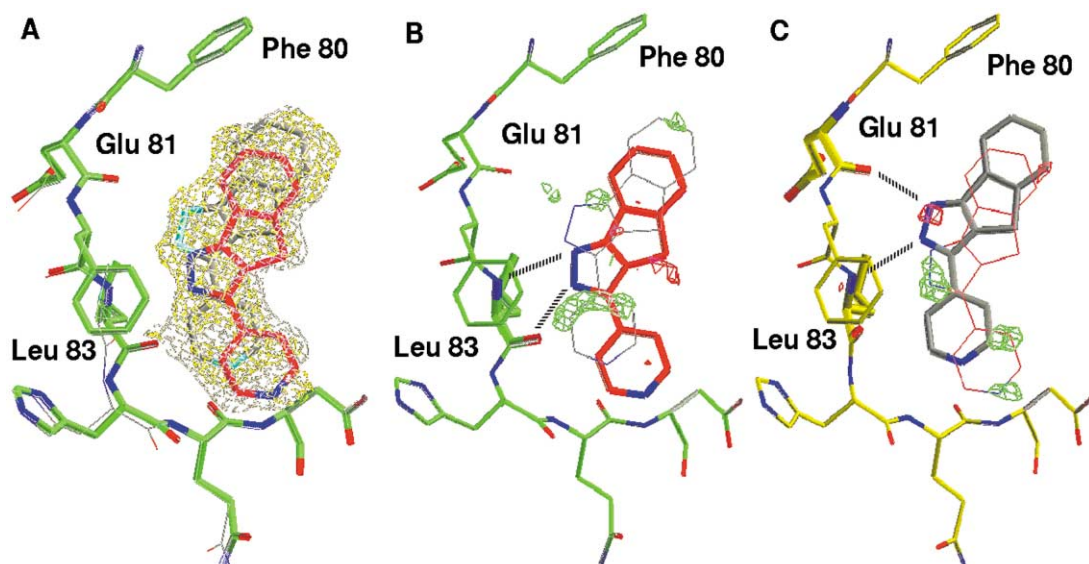


**Figure 4.** (A) Refinement of the two alternate binding modes: final  $\sigma_A$ -weighted 2Fo-Fc,  $\phi_{\text{calc}}$  electron density map (white;  $1\sigma$  contour) and  $\sigma_A$ -weighted 2Fo-Fc,  $\phi_{\text{calc}}$  SA-omit map (yellow;  $0.75\sigma$  contour; both inhibitor molecules were removed from the model, as well as all residues within  $3.5\text{ \AA}$ ). Note that two alternate conformations were refined for protein residues 81–85 (shown here in bold and thin trace), but structural differences are minimal (see text). (B) Refinement of designed binding mode only: residual  $\sigma_A$ -weighted Fo-Fc,  $\phi_{\text{calc}}$  electron density when only the binding mode shown in bold magenta is modeled, with an occupancy of 1.0 (green:  $+3\sigma$  contour; red:  $-3\sigma$  contour). (C) Refinement of second binding mode only: residual  $\sigma_A$ -weighted Fo-Fc electron density when only the binding mode shown in grey is modeled, with an occupancy of 1.0 (green:  $+3\sigma$  contour; red:  $-3\sigma$  contour).

same residue (Fig. 4b). In the second binding mode, N2 of the pyrazole ring donates a H-bond to the carbonyl oxygen of Glu 81, and N1 receives a H-bond from the amide nitrogen of Leu 83 (Fig. 4c). Hence, the observed binding modes involve two distinct tautomeric forms of PKF049-365, differing by the presence of a proton on either N1 or N2 of the pyrazole ring of the inhibitor (Fig. 3). Refinement of the occupancies indicates that the two binding modes are equally populated. Furthermore, switching from one to the other binding mode only requires a small translation/rotation of the inhibitor molecule within the same plane and is not associated with any significant structural rearrangement of the kinase. Two alternate conformations were modelled for residues 81–85 of the hinge region, but only a few minor, structural changes are observed, notably for Leu 83 and His 84. The largest structural difference is observed for the oxygen carbonyl atom of Leu 83, for which the two alternate positions are  $1.6\text{ \AA}$  apart (Fig. 4a–c).

### Conclusion

The work reported in this letter exemplifies the value of structure-based design combined with database mining and experimental structure determination for the identification of lead structures. In addition, it provides an interesting and, to the best of our knowledge, unique example of duality, due to tautomerism, in the binding mode of an enzyme inhibitor.

### Acknowledgements

We thank the BM1A beamline staff at the ESRF, Grenoble (France), for support during data collection.

### References and Notes

- Furet, P.; Meyer, T.; Mittl, P.; Fretz, H. *J. Comput.-Aided Mol. Des.* **2001**, *15*, 489.
- For a review see: Toledo, L. M.; Lydon, N. B.; Elbaum, D. *Curr. Med. Chem.* **1999**, *6*, 775.
- For a review see: Gray, N.; D tivaud, L.; Doerig, C.; Meijer, L. *Curr. Med. Chem.* **1999**, *6*, 859.
- The ligand was designed interactively in MacroModel using the coordinates of PDB structure 1HCK. For the energy minimization of the ligand/CDK2 complex, we employed the AMBER\*/H<sub>2</sub>O/GBSA force field. MacroModel: Mohamadi, F.; Richards, N. G. J.; Guida, W. C.; Liskamp, R.; Lipton, M.; Caufield, C.; Chang, G.; Hendrickson, T.; Still, W. C. *J. Comput. Chem.* **1990**, *11*, 440.
- The substructure search was performed with the Isis Draw-Isis Base software, version 2.1. 3d (MDL). The full Novartis corporate database was searched.
- The CDK2 assay is described in: Soni, R.; Muller, L.; Furet, P.; Schoepfer, J.; Stephan, C.; Zumbstein-Mecker, S.; Fretz, H.; Chaudhuri, B. *Biochem. Biophys. Res. Commun.* **2000**, *275*, 877.
- The CDK1 assay is described in: Riale, V.; Meijer, L. *Anticancer Res.* **1991**, *11*, 1581.
- The available X-ray crystal structures of ligated CDK2 show that the amino acids in contact with the ligands are absolutely conserved in CDK1 (see ref 3).
- PKF049-365 belongs to a series of compounds patented by Novartis (ex-Sandoz) for hypotensive activity: Habeck, D. A.; Houlihan, W. J. *Ger. Offen.* **1973**, DE 2249644.
- Recombinant human CDK2 was produced in baculovirus infected insect cells and purified as described by Russo.<sup>11</sup> Mass spectrometry data of the purified enzyme was consistent with that of full-length, unphosphorylated, wild-type CDK2 with an N-terminal acetyl group. Crystals were grown by vapor diffusion in hanging drops. To this end, a stock solution of CDK2 (6.25 mg/mL) in 10mM Hepes, 15 mM NaCl, pH 7.4 was pre-mixed in a 4:1 ratio with a crystallization solution containing 100 mM Hepes, pH 7.6, 50 mM ammonium acetate, 10% PEG 4,000 and 0.02% sodium azide. After centrifugation, 3  $\mu\text{L}$  droplets were set up on glass cover slips and

equilibrated at room temperature in Linbro plates against the crystallization buffer. Prior to data collection at 120 K, crystals were briefly transferred into a cryo-protectant consisting of 100 mM Hepes, pH 7.6, 50 mM ammonium acetate, 20% PEG 4000 and 20% glycerol. Diffraction data were collected at the European Synchrotron Radiation Facility, beamline BM1A ( $\lambda=0.873$  Å) and processed with the HKL program suite<sup>12</sup> (Table 1). The structure was determined by molecular replacement with AMoRe<sup>13</sup> and refined with X-PLOR 3.851<sup>14</sup> (Table 1). The final model includes protein residues 1 to 36, 44 to 152 and 163 to 298, 267 water molecules and the ligand in two alternate binding modes. The atomic coordinates and the

experimental structure factor amplitudes have been deposited with the Protein Data Bank, with accession code 1JVP.

11. Russo, A.A. In *Methods in Enzymology Cell Cycle Control*; Dunphy, W.G., Ed.; Academic: New York, 1997, Vol. 283, p 3.
12. Otwinowski, Z., Minor, W. In *Methods in Enzymology Macromolecular Crystallography, Part A*; Carter, C. W., Jr., Sweet, R. M., Eds., Academic: New York, 1997, Vol. 276, p. 307
13. Navaza, J. *Acta Crystallogr.* **1994**, A50, 157.
14. Brünger, A.T. In *X-PLOR Version 3.1: A System for X-ray Crystallography and NMR*; Yale University Press: New Haven, 1992.